Scaling Theory of Polyelectrolyte and Polyampholyte Micelles

Nadezhda P. Shusharina and Michael Rubinstein

Department of Chemistry, University of North Carolina, Chapel Hill, North Carolina 27599-3290, USA

1 Introduction

Polymer solutions have been extensively studied for the past three decades [1–3]. Owing to the successful application of scaling theory [1] the solution properties of uncharged polymers are now reasonably well understood. However, many practically important polymers, both synthetic and natural, are charged in polar solvents, most commonly in water. The added complexity of charged systems stems from their long-range electrostatic interactions. The additional emerging length scales make the scaling approach to charged systems much more challenging than for neutral ones. At the same time, research into the functional materials, drug delivery formulations and stabilization of colloidal systems has led to the development of new types of polyelectrolytes, including charged polymeric surfactants. Study of these new polymers is of great industrial importance and provides an excellent opportunity for the introduction and validation of theoretical approaches. Therefore the theory of solutions of charged polymers remains a quickly developing area of polymer physics and material science [4–6].

In contrast to low-molecular weight compounds, polymers have a very important structural degree of freedom called molecular architecture. Specifically, linear polymer chains can be linked together in different fashions forming a single macromolecule. The control of molecular architecture is a widely used approach in the development of polymers with desired properties [7]. The simplest examples of the chain arrangement are block copolymers, where chemically different chains are linked together end to end, and polymer stars, where several chains are linked at one point. The conformations of polymer subchains in a branched molecule depend on its architecture. For example, the interaction of monomers in a star is stronger than in a linear chain because of the additional interactions between the monomers belonging to different chains (arms). If, for example, the monomers along the chain repel each other, the arms in a star will be more extended than the equivalent linear chains [8].

The structure of polyelectrolyte stars is even more complex [9]. An accumulation of a large charge in a small volume of the star leads to a non-uniform distribution of counterions in solution. The non-uniformity is due to an interplay of the electrostatic energy of the star and the entropy of the counterions. To lower the electrostatic energy, counterions tend to be confined within the volume of the star. However, complete confinement (condensation) of counterions would lead to a significant loss of their entropy, so the minimum of the free energy is achieved when a fraction of counterions resides within the star, while the remaining counterions are spread throughout the surrounding solution [10,11]. The uncompensated charge of the star leads to a larger extension of the star arms as compared to neutral stars. Moreover, this extension is not uniform because of the existence of two characteristic regions in the star. In the center the concentration of monomers is so high that the short-range monomer-monomer interactions are stronger than the electrostatic long-range interactions. Hence, in the center the extension is the same as in a neutral star. In the outer region the electrostatics dominate, making the extension much larger than that in the corresponding part of a neutral star.

The general models developed for star-branched macromolecules can be successfully applied to macromolecular aggregates of similar size and geometry. For example, star-like structures may be formed not only by grafting of polymer chains to a small colloidal particle, but as a result of the self-assembly of linear chains. The most familiar case of self-assembly is the formation of micelles, driven by the surface tension at the boundary between solvophobic and solvophilic parts of amphiphilic molecules [12, 13].

Block copolymers [14,15] form micelles when monomers of different blocks have a different affinity for the solvent. In this case, blocks tend to segregate, forming finite-size micelles in solution. A micelle usually has a spherical dense core made of insoluble blocks and a corona consisting of soluble blocks. Many types of water-soluble polymers are charged, so polyelectrolyte blocks are a convenient choice for stabilizing aqueous solutions of polymeric micelles. As part of a block copolymer chain, each charged block is grafted onto the surface of the micellar core, so the structure of the corona resembles that of a polyelectrolyte star. However, the number of arms in the corona is not fixed as in a star, but is equal to the aggregation number of the micelle. It is determined by the balance between the attraction of the uncharged hydrophobic blocks and the repulsion of the charged ones.

The first systematic study of polyelectrolyte micelles was published more than twenty years ago [16]. Since then, micellar solutions of various block copolymers have been investigated. For example, the hydrophobic block could be polystyrene (PS) or poly-*tert*-butylstyrene (PtBS), and the polyelectrolyte block could be poly(acrylic acid) (PAA) or poly(sodium styrenesulfonate) (NaPSS) [17–20]. Theoretical predictions of the equilibrium structure of the micelles have been described in several works [21–24].

While in polyelectrolytes all dissociated groups are like-charged, polyampholytes bear groups of opposite charge on the same chain. There has been

considerable interest recently in polyampholytes both in solution and adsorbed on surfaces [25]. The major feature of polyampholytes is the controllable magnitude and *sign* of the charge of these molecules. The charge of polyampholytes is determined by the relative fraction of positively and negatively charged groups and can be adjusted during synthesis and, in the case of weak polyelectrolytes, by the variation of solution pH [26, 27]. The net charge governs the conformation of a polyampholyte: highly charged chains are in their extended conformations, whereas weakly charged chains form compact colloid-like globules. Increasing polymer concentration in solutions of such globules leads to aggregation of the chains and precipitation. Most of the studies concerning polyampholytes deal with randomly distributed oppositely charged groups within a chain. Much less attention has been paid to the case of block polyampholytes where the opposing charges are grouped in long sequences. Several recent experimental works report micelle formation in solutions of diblock polyampholytes (diblock copolymers with a positively and a negatively charged block) [28, 29]. In such micelles, oppositely charged blocks collapse in the micellar core. The blocks carrying the uncompensated charge are in the corona, stabilizing the micelle in solution. Micellization in diblock polyampholyte solutions has been considered theoretically [30, 31].

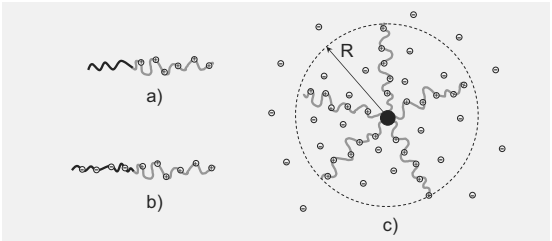

Fig. 1. Sketch of (a) a diblock copolymer with one uncharged and one polyelectrolyte block; (b) a diblock polyampholyte; (c) a spherical star-like micelle or a star of radius R and its counterions.

Below we review a scaling description of polyelectrolyte micelles in solutions of (i) diblock copolymers with an uncharged and a polyelectrolyte block, and (ii) diblock polyampholytes, see Fig. 1. In both cases the solvent is a polar medium (e.g., water) with dielectric permittivity ε at temperature T. The shell (corona) of these micelles is composed of polyelectrolyte chains and therefore the energy of the shell is the same as the energy of a polyelectrolyte star (as long as the corona is much larger than the micellar core). The equilibrium micellar aggregation number is defined from the free energy balance between the core and the corona. We will start our review with the theory of polyelectrolyte stars and then continue with the specific features resulting from different interactions of the core.

The chapter is organized as follows. In the next section the scaling description of a single polyelectrolyte chain will be briefly outlined [1, 32]. The main results for polyelectrolyte stars will be presented in Sect. 3. In Sect. 4 the theory for polyelectrolyte micelles will be reviewed according to the papers [21, 22] and Sect. 5 will be dedicated to the theory of polyampholyte micelles [30, 31].

2 Scaling Description of Polyelectrolyte Chains

Let us briefly recall the scaling description of a single polyelectrolyte chain in a dilute salt-free solution. These chains are stretched due to the intra-chain electrostatic repulsion. The conformation of the chain can be described as a linear array of electrostatic blobs [1, 32]. The size of the electrostatic blob ξ_{el} is determined by the condition that the energy of electrostatic interaction between two neighboring blobs along the chain is of the order of the thermal energy:

$$\frac{e^2 f^2 g_{el}^2}{\varepsilon \xi_{el}} \approx k_B T. \tag{1}$$

Here e is the elementary charge, g_{el} is the number of monomers in a blob, k_B is the Boltzmann constant, and T is the absolute temperature (we keep our discussion at the level of scaling approximation and omit numerical coefficients). The statistics of the chain is unperturbed by the electrostatic interactions on a length scale smaller than the electrostatic blob size. It is determined by the short-range interactions between monomers in solution. We will consider the case of a θ-solvent [1] where the monomers interact via three-body repulsion. The statistics of a chain in a θ-solvent is almost Gaussian, hence the size of the electrostatic blob ξ_{el} is related to the number of monomers g_{el} in it as $\xi_{el} \approx b g_{el}^{1/2}$ and substituting this relation into (1) one concludes that

$$\xi_{el} \approx b(uf^2)^{-1/3}, \tag{2}$$

where $u = l_B/b$ is the ratio of the Bjerrum length

$$l_B = \frac{e^2}{\varepsilon k_B T} \tag{3}$$

to the Kuhn length b [2, 3]. The Bjerrum length is a measure of the strength of the electrostatic interactions. It is equal to the distance at which the interaction between two elementary charges in the medium with the dielectric constant ε is of the order of $k_B T$.

For flexible polymers in an aqueous solution, $b \approx 1$nm, $T \approx 300$K, $\varepsilon \approx 80$, and the parameter u is approximately equal to unity.

The energy of a polyelectrolyte in the elongated conformation is of the order of the thermal energy $k_B T$ per electrostatic blob

$$\frac{F_{polyel}}{k_BT} \approx \frac{N}{g_{el}} \approx N(uf^2)^{2/3}. \tag{4}$$

The length of the polyelectrolyte chain is estimated as $R_{polyel} \approx \xi_{el} N/g_{el}$ and, using (2) we get

$$R_{polyel} \approx bN(uf^2)^{1/3}. \tag{5}$$

In the next section we will consider the conformations of a star polymer consisting of a fixed number of polyelectrolyte arms, see Fig. 1c.

3 Polyelectrolyte Stars

3.1 Free Energy of the Star

Let us consider a dilute solution of polyelectrolyte stars composed of p identical arms. We will assume that the arms are flexible chains of N Kuhn segments of length b, and the non-coulombic interactions between the segments correspond to a θ-condition. The net charge of an arm (counted in the elementary charge units e), or the valence is

$$Z_{net} = Nf, \tag{6}$$

where f is the fraction of charged monomers in an arm. Correspondingly, there are pNf monovalent counterions per star in the solution.

The counterions are distributed between the volume of the star and the volume of solution not occupied by the stars, i.e. fraction α of them is freely floating in the solution and fraction $1-\alpha$ is confined within the volume of the star, reducing its charge. This confinement is one of two types of counterion condensation called spherical condensation [33]. The counterions within a sphere surrounding a star remain osmotically active. If the linear charge density along the arms of the star is higher than approximately one elementary charge per Bjerrum length (3), the counterions condense into the close vicinity of each arm and practically lose their translational entropy [34, 35]. This case, called cylindrical (Manning) condensation, can be achieved for polymers with a higher fraction of charged monomers f in solvents with lower dielectric constant, or for multivalent counterions. In the following description we will restrict our consideration to the case with only spherical condensation and assume no cylindrical condensation.

The radius of the star R depends on the uncompensated (effective) charge of the star $eZ_{eff} = epZ_{net}\alpha$. Both the equilibrium radius and the effective charge of the star can be found by minimizing the free energy of the star with respect to R and α.

The electrostatic self-energy per arm of the star with effective charge eZ_{eff} and radius R is

$$\frac{F_{el}}{k_BT} \approx l_B \frac{pZ_{net}^2\alpha^2}{R}. \tag{7}$$

The contribution to the free energy per arm due to the elasticity of an arm is related to conformational entropy losses in a stretched chain [3, 11]

$$\frac{F_{str}}{k_BT} \approx \frac{R^2}{Nb^2}. \tag{8}$$

The entropic part of the free energy per arm due to counterions is

$$\frac{F_{count}}{k_BT} \approx Z_{net}(1-\alpha)\ln\left(\frac{pZ_{net}(1-\alpha)}{R^3}\right) + Z_{net}\alpha\ln(f\alpha cb^3), \tag{9}$$

where c is the average monomer concentration in the solution. The two terms in (9) are the entropic part of the free energy per arm due to counterions confined into the volume of the star and to free counterions, respectively.

3.2 Polyelectrolyte and Osmotic Regimes

The limit $\alpha \approx 1$ corresponds to the polyelectrolyte regime where most of the counterions are in the surrounding solution and the effective charge of the star is very close to the net charge. Then, the electrostatic energy per arm of the star is determined by the effective charge of the star, which is approximately equal to its total net charge epZ_{net}:

$$\frac{F_{el}^{PE}}{k_BT} \approx l_B\frac{pZ_{net}^2}{R}. \tag{10}$$

The equilibrium size of the star is determined by minimizing the sum of the energy of electrostatic repulsion between arms (10) and the elastic energy (8) with respect to the star size R:

$$R_{PE} \approx bp^{1/3}N(uf^2)^{1/3}. \tag{11}$$

The extension of the star arms is larger than the extension of a free polyelectrolyte chain R_{polyel}, see (5), because of the additional stretching of the arms in the star caused by the inter-chain electrostatic repulsion. Each arm of the star can be represented as a sequence of "tension" blobs [3] of the size:

$$\xi_t \approx \frac{b^2N}{R_{PE}} \approx bp^{-1/3}(uf^2)^{-1/3} = \frac{\xi_{el}}{p^{1/3}}. \tag{12}$$

The fraction of free counterions α in the polyelectrolyte regime depends on the star concentration. Indeed, the volume accessible to free counterions is not infinite but of the order of the cube of the distance between the stars in solution. In the polyelectrolyte regime the following expressions for α can be written [21]:

$$\alpha = 1 - \phi_{star}e^U \quad \text{if} \quad 1-\alpha \ll 1, \tag{13}$$

where $\phi_{star} \approx R^3c/pN$ is the volume fraction occupied by stars in the solution and the dimensionless potential of the star U is equal to

$$U \equiv l_B \frac{pZ_{net}}{R}. \tag{14}$$

The physical interpretation of the parameter U is the energy of electrostatic interaction between the charged star and a counterion located at the periphery of the star (specifically at the distance R from the center of the star) divided by the thermal energy k_BT. The counterions can be considered as "free" if $U \ll 1$, i.e. if the entropy loss due to confinement of a counterion inside the star is larger than the energy gain due to the reduction of the electrostatic repulsion.

The scaling estimate of the size of the charged star in the polyelectrolyte regime (11) assumed uniform stretching of the star arms. The conformation of an arm is thought of as a string of tension blobs of equal size given by (12). To calculate the radial distribution of monomers in the star more precisely, one has to consider the balance of forces acting on the section of a star arm. Such calculations have been done for an individual polyelectrolyte chain [32,36,37]. It was shown that in a chain of finite length the monomers are distributed non-uniformly and the chain has a trumpet-like conformation with blob size increasing from the middle point to the ends [36, 37]. The inhomogeneity occurs because the electrostatic potential is smaller near the ends where the charges have fewer neighbors. The increase of the blob size towards the ends is however slow and the correction to the size of the chain obtained by simple scaling estimations is logarithmic. These predictions of the scaling model have been confirmed by Monte Carlo simulations [37]. The technique developed in [32, 36] can be applied to model non-uniform stretching of arms in an individual polyelectrolyte star [33]. Here, the arms have a conformation of a half trumpet with the tension blob size logarithmically increasing from the center to the periphery of the star.

At the crossover between the regime of mostly free counterions ($\alpha \approx 1$) to the regime of mostly confined counterions ($\alpha \ll 1$) the electrostatic potential of the star is of the order of the thermal energy k_BT, i.e. the parameter $U \approx 1$. For this value of the electrostatic potential the tension blob size ξ_t (12) is equal to the distance between charges along the chain. Thus, the free energy loss due to chain stretching is of the order of the thermal energy k_BT per charge, i.e., the same as the entropy gain per counterion released from the star. Above this crossover the excess counterions start condensing on the star and the solution of stars is said to be in the *osmotic* regime [11]. The parameter α in the osmotic regime can be approximated as [21]

$$\alpha = \frac{1}{U} \ln \frac{1}{\phi_{star}} \quad \text{if} \quad \alpha \ll 1 \tag{15}$$

The stretching force in the osmotic regime is dominated by the entropy of the confined counterions and is usually referred to as the osmotic contribution to the free energy of the star

$$\frac{F^{OS}_{count}}{k_BT} \approx Z_{net} \ln \left(\frac{pZ_{net}b^3}{R^3} \right). \tag{16}$$

Balancing this confinement entropy of counterions with the elastic energy of the arm, see (8), we obtain the equilibrium size of the star in the osmotic regime:

$$R_{OS} \approx bNf^{1/2}, \tag{17}$$

which is independent of the number of arms in the star. The size of the tension blob in the osmotic regime corresponds to one charge per blob:

$$\xi_t \approx bf^{-1/2}. \tag{18}$$

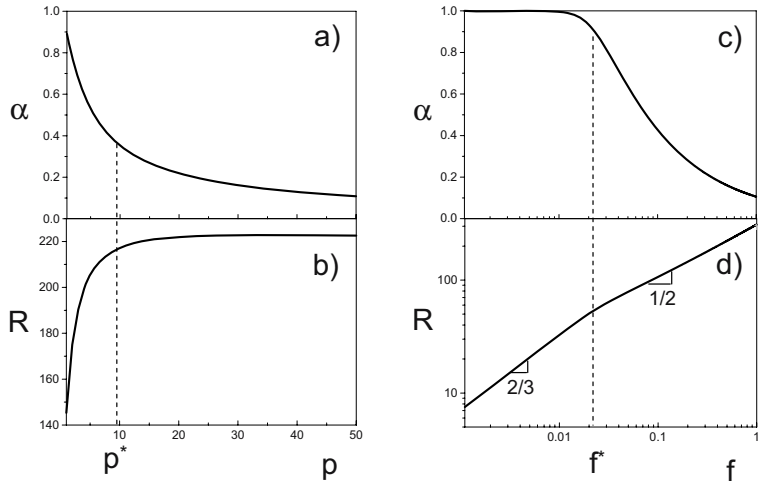

Fig. 2. (a) The fraction of counterions released from the star α, and (b) the radius of the star R as functions of the number of arms in the star p; (c) the fraction of counterions released from the star α, and (d) the radius of the star R as functions of the fraction f of charged monomers in an arm. The fixed parameters are $N = 250$, $u = 1.5$, $f = 0.5$ in (a) and (b), $p = 30$ in (c) and (d).

Let us comment on the monomer distribution in the osmotic regime. An exact solution of the Poisson–Boltzmann equation coupled to the chain elasticity is available for the planar osmotic brush [11]. It was demonstrated that at equilibrium the counterions are confined within the brush in the osmotic regime preserving the local electroneutrality. The loss of the counterion entropy is compensated by the gain of the electrostatic energy. The local electroneutrality is achieved by the local concentration of counterions proportional to the concentration of polymer segments.

In the spherical geometry, similar effects have been observed by solving the Poisson–Boltzmann equation numerically [38] and by Monte Carlo simulations [39]. These theoretical approaches predict that the density profiles of the monomers and counterions closely follow each other inside the star. This finding is confirmed by experiments using small angle neutron scattering [40].

The dependencies of α and R on the number of arms p and the fraction of charged monomers f are shown in Fig. 2. These dependencies are obtained by minimizing the free energy of the star with the contributions given by (7), (8), and (9). The fraction of free counterions decreases with increasing bare charge of the star at the expense of increased fraction of confined counterions. At the same time the slope of the dependence of the star radius changes indicating the crossover from the polyelectrolyte to the osmotic regime. The crossover values p^* and f^* can be obtained from the condition $U = 1$ in (14)

$$p^* \approx u^{-1} f^{-1/2} \tag{19}$$

$$f^* \approx u^{-2} p^{-2}. \tag{20}$$

The polyelectrolyte regime is realized at $p < p^*$ (Fig. 2a,b) or at $f < f^*$ (Fig. 2c,d). The osmotic regime appears at higher values of p and f.

4 Polyelectrolyte Micelles

The results obtained in the previous section can be used to calculate the equilibrium aggregation number of spherical star-like micelles made of diblock copolymers with one uncharged and one polyelectrolyte block. Let us consider a diblock copolymer with N_0 monomers in the uncharged block and N monomers in the polyelectrolyte block. Both blocks are flexible polymers with the same Kuhn segment length b. To ensure micellization, monomers of the neutral block are solvophobic (hydrophobic) and their interaction is described by the temperature-dependent excluded volume parameter [3]

$$v \approx \frac{T - \theta}{T} b^3, \tag{21}$$

where the deviation from the θ-temperature is negative in a poor solvent indicating effective attraction between monomers.

The non-electrostatic interactions of monomers of the polyelectrolyte block are θ-like and the fraction of charged monomers in it is f, so the chain carries the net charge $eZ_{net} = eNf$.

4.1 Unimers

The uncharged block in a selective solvent collapses into a globule leading to a tadpole conformation of the whole chain with a neutral globular head and a polyelectrolyte tail. The conformation of the collapsed block is described by a dense packing of the thermal blobs of size [3]

$$\xi_T \approx \frac{b^4}{|v|} \tag{22}$$

The density of the globule is proportional to the excluded volume parameter v (21) and its size is

$$R_{gl} \approx b\frac{N_0^{1/3}}{|v|^{1/3}}. \tag{23}$$

Each thermal blob inside the globule is attracted to a neighboring blob with the energy of the order of the thermal energy k_BT. Thus, in the framework of the scaling approach the bulk contribution to the free energy of a globule F_{gl} is proportional to the number of thermal blobs in the neutral block $N_0/g_T \approx N_0|v|^2/b^6$.

In addition to the bulk free energy, the globule has a surface free energy contribution due to the polymer-solvent interface. The origin of this term is the difference between the number of nearest neighbors of a blob inside the globule and on its surface. The surface energy can be estimated as the thermal energy k_BT per blob at the surface of the globule [3]:

$$\frac{F_{surf}^{uni}}{k_BT} \approx \frac{R_{gl}^2}{\xi_T^2} \approx N_0^{2/3}|v|^{4/3}. \tag{24}$$

The electrostatic self-energy of the tadpole tail and the length of the tail are given by (4) and (5), respectively.

4.2 Micelles

Aggregation in solutions of neutral-polyelectrolyte diblock copolymers is driven by the attraction between the heads of the tadpoles. By bringing the heads of two tadpoles together, one reduces the energy of the polymer-solvent interface. The stabilizing factor which prevents the formation of an infinite aggregate with increasing polymer concentration is the electrostatic repulsion between tails. The possibility of micellization is determined by the entropy of the tadpoles. The micelles are formed at solution concentrations higher than the critical micelle concentration (cmc) [12].

The aggregation number of micelles is controlled by the balance between the surface energy of the uncharged micellar core and the electrostatic repulsion between the charged blocks in the corona.

The radius of the core is (cf. (23))

$$R_{core} \approx bp^{1/3}N_0^{1/3}|v|^{-1/3}, \tag{25}$$

and the surface energy per chain of a micelle formed by p diblock copolymers is

$$\frac{F_{surf}}{k_BT} \approx \frac{R_{core}^2}{p\xi_T^2} \approx p^{-1/3}N_0^{2/3}|v|^{4/3}. \tag{26}$$

As in dilute solutions of polyelectrolyte stars, both polyelectrolyte and osmotic regimes can be observed in the micellar solution depending on the net charge of chains forming the micelle.

Polyelectrolyte Regime (Free Counterions, $\alpha \approx 1$)

Substituting (11) into the expression for the electrostatic energy of the corona (10) we obtain the electrostatic contribution to the total energy of the micelle per chain:

$$\frac{F_{el}^{PE}}{k_B T} \approx p^{2/3} N (uf^2)^{2/3}. \tag{27}$$

The aggregation number in the polyelectrolyte regime is determined by the balance of this electrostatic free energy of the corona and the surface free energy of the core (26):

$$p_{PE} \approx \frac{N_0^{2/3} |v|^{4/3} f}{Z_{net} (uf^2)^{2/3}}. \tag{28}$$

Note that all contributions to the total free energy of the micelle, namely F_{surf} (26), F_{el} (27) and F_{str} (8) are balanced at equilibrium ($F_{surf} \approx F_{el} \approx F_{str}$).

Osmotic Regime (Condensed Counterions, $\alpha \ll 1$)

The aggregation number in the osmotic regime is estimated by balancing the surface energy of the core (26) and the osmotic term of the free energy, see (16), which leads to

$$p_{OS} \approx \frac{N_0^2 |v|^4}{Z_{net}^3}. \tag{29}$$

At the crossover between the polyelectrolyte and osmotic regimes the two free energy contributions F_{PE} (27) and F_{OS} (16) are of the same order of magnitude and the micellar aggregation numbers given by (28) and (29) are equal. The net valence Z_{net}^* per one chain of the micelle at this crossover is

$$Z_{net}^* \approx \frac{N_0^{4/5} u^{2/5} |v|^{8/5}}{N^{1/5}}. \tag{30}$$

In Fig. 3 we have plotted the aggregation number p as a function of the net valence of the diblock copolymer chain. Diblock copolymers with a low valence ($Z_{net} < Z_{net}^*$) form polyelectrolyte micelles (regime PE), whereas strongly charged chains ($Z_{net} > Z_{net}^*$) attract more counterions into the corona and the equilibrium micelles formed by these highly charged copolymers are in the osmotic regime (OS). As the charge of polyelectrolyte block is increased, aggregation of unimers into micelles becomes unfavorable. For the micelle to be formed, the surface energy of the unimer head has to be larger than the entropy of the counterions per chain being confined inside the osmotic micelle. Micelles would not form if bringing block copolymers together led to the loss of counterion entropy larger than the decrease in the surface energy of the aggregate. The maximum net charge at which the aggregation is still possible is determined by the condition

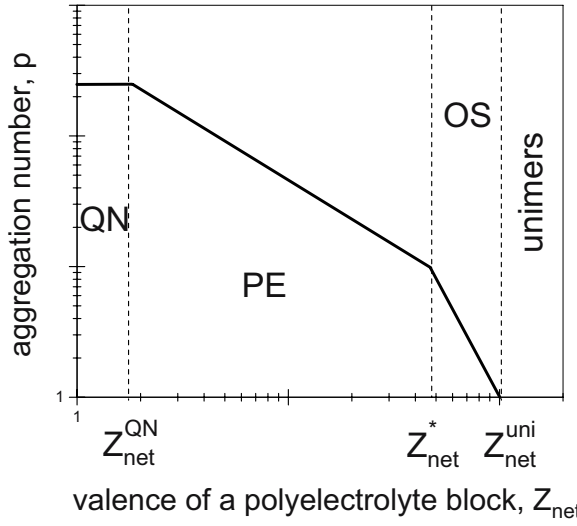

Fig. 3. The aggregation number of micelles formed by neutral-polyelectrolyte diblock copolymers as a function of the net valence per chain $Z_{net} = Nf$. The parameters are: $N_0 = 1000$, $f = 0.01$, $u = 1$.

$$Z_{net}^{uni} \approx N_0^{2/3}|v|^{4/3}. \tag{31}$$

The aggregation number in the polyelectrolyte regime increases with decreasing polyelectrolyte block charge eZ_{net} leading to the increase of the monomer concentration in the corona. At $Z_{net} = Z_{net}^{QN}$, see Fig. 3, non-electrostatic short-range interactions between monomers become more important than the long-range electrostatic interactions. The aggregation number of the micelles at small Z_{net} is determined by the minimization of the surface free energy and the energy of the arm stretching due to the short-range inter-arm repulsion [8]. However, such quaisi-neutral micelles (regime QN in Fig. 3) may become unstable. Since the neutral blocks in the core are "grafted" onto the surface of the core they become stretched. If the stretching free energy of a block in the core is of the order of the difference between the free energy of the corona and the surface free energy per chain, the spherical geometry of the core is unfavorable leading to shape transitions into cylindrical and planar aggregates [24, 41].

4.3 Critical Micelle Concentration

Experimental data suggest that micelle formation in solutions of block copolymers is a reversible process with a rather sharp transition between the two states: the solution of unimers and the solution of micelles [42–45]. There is a phase equilibrium (coexistence) of the two states at the critical micelle concentration (*cmc*). Therefore, the chemical potentials of a free chain (unimer) and

of a chain in the micelle of equilibrium size are equal. Below we consider the equilibrium between unimers and the micelles of the two types, polyelectrolyte and osmotic.

In the polyelectrolyte regime, aggregation is governed by competition between the loss of entropy of chains aggregated into the micelle and the energetic gain due to reduction of the surface energy of the micelle (the entropy of the counterions is the same in the solution of unimers and micelles because there is no condensation in the polyelectrolyte regime). The difference in the surface energies of the unimer, see (24), and of the equilibrium micelle, see (26), can be approximated by the unimer contribution, since $F_{surf} \approx p_{PE}^{-1/3} F_{surf}^{uni}$ and $p_{PE} \gg 1$. The *cmc* in the polyelectrolyte regime can be estimated as:

$$c_{cmc} b^3 \approx \exp\left(-\frac{F_{surf}^{uni}}{k_B T}\right) \approx \exp\left(-N_0^{2/3} |v|^{4/3}\right) \tag{32}$$

In the case of the osmotic micelles, the main contribution of the free energy change is related to the entropy loss of counterions, as they are localized within the micellar volume. In this case the counterion entropy loss is compensated by the surface energy gain due to the aggregation of chains into micelles. This leads to the following expression for the critical micelle concentration

$$c_{cmc} b^3 \approx c_{mic} \exp\left(-\frac{1}{Z_{net}} \frac{F_{surf}^{uni}}{k_B T}\right) \approx \frac{pN}{R^3} \exp\left(-\frac{N_0^{2/3} |v|^{4/3}}{Z_{net}}\right), \tag{33}$$

where $c_{mic} = pN/R^3$ is the monomer concentration inside the micelle. The fact that the counterions become confined when unimers aggregate to form the osmotic micelle greatly increases the *cmc* (note the factor $1/Z_{net}$ in the exponential).

In a more precise consideration one should take into account a small but finite fraction of counterions (1- α) $\ll$1 localized in a star in the polyelectrolyte regime. If the number of localized counterions per chain in a micelle Nf(1-α) is larger than unity then the critical micelle concentration is controled by the entropy of counterions, since the entropy loss due to confinement of the counterions exceeds the entropy loss due to confinement of free chains into a micelle.

4.4 Effect of Added Salt

Salt ions screen the electrostatic interactions and thus an addition of low-molecular-weight salt essentially influences the equilibrium properties of solutions of polyelectrolyte micelles, see [46] and references therein. The effect of salt on solutions of aggregated polyelectrolytes is more complex than that on solutions of free polyelectrolytes due to strong inter-chain interactions and the phenomenon of counterion condensation in micelles.

Addition of salt to grafted polyelectrolyte layers leads to a decrease in the layer thickness because of weakening of the chain stretching [11, 23]. The stretching reduces upon screening of the inter-chain electrostatic repulsion between densely grafted chains.

The screening effects in micellar systems result in increasing aggregation number [23]. Since the repulsion between the corona chains weakens, the free energy per chain in a micelle decreases and therefore larger micelles can be formed. The size of the micellar corona decreases slower than the thickness of the layer with a fixed number density of grafted chains due to the increase of the aggregation number with salt concentration. The increasing aggregation number leads to decreasing inter-chain separation and thus to stronger chain stretching. At the same time, however, the stretching weakens due to an enhanced screening. These predictions, based on the scaling arguments, [23] are in good agreement with the experimental data [46].

5 Polyampholyte Micelles

Star-like micelles can be formed in solution of diblock copolymers with oppositely charged blocks. Both aggregation and stabilization of these micelles are governed by the electrostatic interactions. Consider a diblock polyampholyte chain consisting of N segments, N_+ in the positively charged block and N_- in the negatively charged block, $N = N_+ + N_-$. The short-range non-electrostatic interactions between segments are assumed to be θ-like. The fractional charge of the two blocks is assumed to be the same, $f_+ = f_- = f$. Therefore, the net charge of the chain eZ_{net} is related to the block length asymmetry $\Delta N = N_+ - N_-$ according to

$$eZ_{net} = e\Delta N f \tag{34}$$

For definiteness, we assume that $N_+ > N_-$, so that $\Delta N > 0$.

5.1 Unimers

The conformation of a diblock polyampholyte chain depends on the block charge asymmetry, or the net charge Z_{net}. Chains with high charge asymmetry ($\Delta N \approx N$) are elongated similar to polyelectrolyte chains, see Sect. 2. On the contrary, if the diblock polyampholyte chain is nearly charge-symmetric ($\Delta N \ll N$), it collapses into a globule, see Fig. 4a. The collapse is driven by the charge density fluctuation-induced attraction [47, 48] between oppositely charged blocks. The equilibrium density of the globule is determined by the balance between fluctuation-induced attraction and three-body repulsion (in the case of a θ-solvent). There is an important length scale in the globule called the correlation length ξ. Polymer statistics at the length scale smaller than the correlation length is unperturbed by the fluctuation-induced attractive interactions. This leads to the usual θ-solvent scaling relation between the

correlation length ξ and the number of monomers g in the correlation blob, $\xi \approx bg^{1/2}$. At length scales larger than the correlation length, attractive interactions result in dense packing of the correlation blobs. The local structure of the "melt" of blobs resembles that of a concentrated solution of positively and negatively charged polyelectrolytes with each blob being predominantly surrounded by oppositely charged blobs, see Fig. 4. The electrostatic interactions between any two neighboring blobs are of the order of the thermal energy k_BT:

$$k_BT\frac{l_Bf^2g^2}{\xi} \approx k_BT. \tag{35}$$

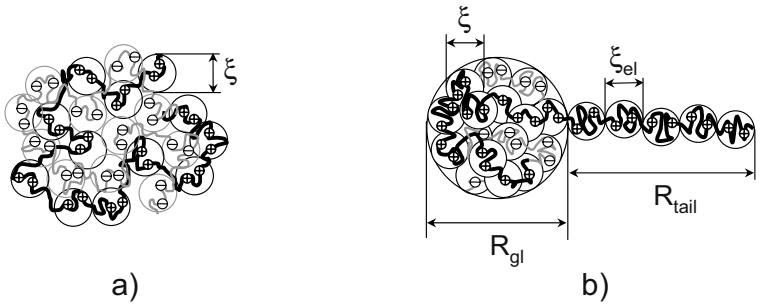

Fig. 4. Blob picture of (a) a charge-symmetric polyampholyte globule. A correlation volume (blob) containing a section of positively charged chain is predominantly surrounded by blobs containing sections of negatively charged chains. (b) A tadpole conformation of a charge-asymmetric unimer with head size R_{gl} and tail length R_{tail}. $\xi \approx \xi_{el}$ is the correlation blob size. Reproduced from [31]. Copyright (2005) American Chemical Society.

The blob size ξ is, therefore, determined by a condition similar to that controlling the size of an electrostatic blob, cf. (1). However, in the case of charge-symmetric polyampholytes, the neighboring blobs are predominantly oppositely charged, reflecting the attractive nature of intra-chain interactions. Qualitatively, the typical length scale of the repulsive electrostatic interactions in strongly charge-asymmetric block polyampholyte chains – electrostatic blob size ξ_{el} (2) is the same as the length scale of the attractive interactions in charge-symmetric polyampholytes

$$\xi \approx \xi_{el}. \tag{36}$$

The correlation blobs inside the globule are space filling, therefore the local monomer concentration is

$$c_{gl}b^3 \approx \frac{b^3g}{\xi^3} \approx \frac{b}{\xi} \approx (uf^2)^{1/3}, \tag{37}$$

which determines the size of the globule

$$R_{gl} \approx \left(\frac{N}{c_{gl}}\right)^{1/3} \approx bN^{1/3}(uf^2)^{-1/9}. \tag{38}$$

The volume contribution to the free energy of the globule is proportional to the number of its constituent blobs:

$$\frac{F_{gl}}{k_BT} = -\frac{N}{g} \approx -\frac{Nb^2}{\xi^2} \approx -N(uf^2)^{2/3}. \tag{39}$$

This free energy is of the same order of magnitude as the electrostatic energy of a polyelectrolyte chain (4) and the minus sign reflects the attractive nature of the intra-chain interactions.

The surface energy can be estimated as the thermal energy k_BT per correlation blob on the surface of the globule [3]:

$$\frac{F_{surf}^{uni}}{k_BT} \approx \frac{R_{gl}^2}{\xi^2} \approx N^{2/3}(uf^2)^{4/9}. \tag{40}$$

At the intermediate charge asymmetries, block polyampholyte chains adopt a tadpole conformation, see Fig. 4b. The head is formed by all of the negatively charged monomers and a compensating amount of the positively charged monomers. The remaining ΔN monomers form the tail. The charge of the head is nearly zero, so the total net charge eZ_{net} of the chain is carried by ΔNf charged monomers in the tail. For a high enough valence of the diblock Z_{net} (see the discussion in [31]) the radius of the head, given by (38) is much smaller than the length of the tail (cf. (5))

$$R_{tail} \approx b\Delta N(uf^2)^{1/3}. \tag{41}$$

Next, we will consider micellization in dilute solutions of the tadpoles and discuss how the net charge per chain Z_{net} influences micellar structure.

5.2 Star-Like Micelles

The aggregation in solutions of block polyampholytes is driven by the charge density fluctuation-induced attractive interactions between oppositely charged blocks. The unimers start to aggregate above the *cmc* to reduce the surface tension at the boundary between the collapsed blocks and the solvent.

A novel feature of the polyampholyte micelles is the possibility of partitioning of the chains between the core and the corona. Indeed, in the case of micelles formed by diblock copolymers with one hydrophobic and one polyelectrolyte block, the core is formed exclusively by the hydrophobic blocks. In the micelles of diblock polyampholytes, both positively and negatively charged blocks form the core. The corona is formed by the excess of blocks with higher charge (in our model, positively charged), but this excess can be partitioned

in different ways. One possible structure is realized when the total net charge of the micelle epZ_{net} is carried by p equivalent tails in the corona, see Fig. 5a. All chains in such micelle are in a similar conformation contributing the same portion of the longer block to the core of the micelle [30]. Such arrangement of polyampholyte chains in the micelle is called the *restricted model*. The structure of such micelles is similar to the structure of the micelles made of diblock copolymers with a hydrophobic and a polyelectrolyte block, described in the previous sections. The main difference is that in the polyampholyte micelles both blocks participate in the formation of the core, and the corona consists not of the entire positively charged block but only of an outer part consisting of ΔN monomers.

In the *unrestricted model* [31] one releases the equipartition constraint allowing some chains to be completely confined to the core of the micelle while the others have the entire stronger charged block in the corona, see Fig. 5b.

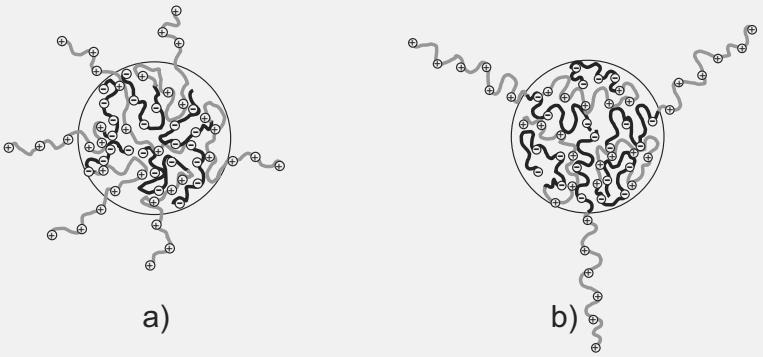

Fig. 5. Sketch of star-like micelles of diblock polyampholytes: (a) a micelle according to the restricted model; (b) a micelle with disproportionated chains according to the unrestricted model. Reproduced from [31]. Copyright (2005) American Chemical Society.

The cores of the micelles with aggregation number p have the same size in the two models

$$R_{core} \approx bp^{1/3}N^{1/3}(uf^2)^{-1/9}, \tag{42}$$

and correspondingly the same surface free energy per chain

$$\frac{F_{surf}}{k_BT} \approx \frac{R_{core}^2}{p\xi^2} \approx p^{-1/3}N^{2/3}(uf^2)^{4/9}. \tag{43}$$

In order to compare the two models one needs to calculate the electrostatic energy associated with the total charge epZ_{net} of the aggregate [31].

Each disproportionated micelle in the unrestricted model is composed of p chains with p' positively charged blocks in the corona and $p - p'$ chains

completely confined to the core, see Fig. 5b. The charge balance in the core:

$$pN_- \approx (p - p')N_+ \tag{44}$$

gives an estimate for the number p' of positively charged blocks in the corona of the micelle

$$p' \approx 2p\frac{\Delta N}{N + \Delta N} \approx p\frac{Z_{net}}{Nf}. \tag{45}$$

Note that if $Z_{net} \ll Nf$, the number of blocks in the corona for the unrestricted model p' is much smaller than in the restricted model ($p' \ll p$). Thus in the restricted model the net charge epZ_{net} is on short sections of all stronger charged blocks. In the unrestricted model the same net charge epZ_{net} is placed on few entire blocks in the corona which makes the electrostatic energy of the disproportionated micelle lower than the electrostatic energy in the restricted model. In the osmotic regime the difference between the two models is also determined by the size of the corona. In the unrestricted model the size is larger than that in the restricted model. This creates a larger volume for the counterions confined in the disproportionated micelle and therefore the entropy loss is smaller compared to the restricted model.

Below we evaluate the energy of the micellar corona according to the unrestricted model in the two regimes of the counterion distribution and calculate the equilibrium aggregation number.

Polyelectrolyte Regime ($\alpha \approx 1$)

The interactions between corona chains in the polyelectrolyte regime are purely electrostatic and the equilibrium size of the corona is determined by the balance of the energy of electrostatic repulsion between chains in the corona, see (10) and their elastic energy due to stretching of these chains to the corona size R. The number of monomers in each of p' corona blocks is $N_+ = N(1 + \Delta N/N)/2 \approx N$. The elastic energy of a star-like micelle per chain (cf. (8)):

$$\frac{F_{str}}{k_BT} \approx \frac{p'}{p}\frac{R^2}{Nb^2} \tag{46}$$

is equilibrated by the electrostatic energy (10) leading to the equilibrium size of the corona

$$R_{PE} \approx bp^{1/3}\Delta N\left(\frac{N}{\Delta N}\right)^{2/3}(uf^2)^{1/3}. \tag{47}$$

Substituting (47) into the expression for the electrostatic energy of the corona (10) we obtain the electrostatic contribution to the total free energy of the micelle per chain in the unrestricted model:

$$\frac{F_{el}^{PE}}{k_BT} \approx p^{2/3}\Delta N\left(\frac{\Delta N}{N}\right)^{2/3}(uf^2)^{2/3}. \tag{48}$$

The aggregation number in the polyelectrolyte regime is determined by the balance of the electrostatic free energy of the corona (48) and the surface free energy of the core (43):

$$p_{PE} \approx \frac{N^{4/3} f^{5/3}}{Z_{net}^{5/3} (uf^2)^{2/9}}. \tag{49}$$

Osmotic Regime ($\alpha \ll 1$)

The aggregation number in this regime is calculated by minimizing the sum of the surface energy of the core (43) and the osmotic term of the free energy (16) which leads to

$$p_{OS} \approx \frac{(uf^2)^{4/3} N^2}{Z_{net}^3}. \tag{50}$$

At the crossover boundary between the polyelectrolyte and osmotic regimes the two free energy contributions F_{PE} and F_{OS} are of the same order of magnitude and the micelle aggregation numbers, given by (49) and (50) are equal to each other resulting in the expression for the crossover between the polyelectrolyte and osmotic regimes

$$Z_{net}^* \approx \frac{N^{1/2}}{f^{5/4}} (uf^2)^{7/6}. \tag{51}$$

The polyelectrolyte regime is realized if the net valence per chain is larger than this crossover value, i.e. at $Z_{net} > Z_{net}^*$, and correspondingly the osmotic regime takes place at smaller Z_{net}. This situation is opposite to the one occurring in solutions of micelles with a hydrophobic core, see Fig. 3. The opposite order of appearance of the regimes is explained by the behavior of the electrostatic potential of the micelle $\approx l_B p Z_{net}/R$ as a function of Z_{net}. The major factor determining the potential is the total charge of the micelle epZ_{net} since the dependence of the micellar radius R on Z_{net} is weak. In both types of micelles the decrease of the valence per chain Z_{net} leads to larger micellar aggregation number p. In polyelectrolyte micelles the aggregation number p grows slower than $1/Z_{net}$ resulting in decrease of the potential. In the case of polyampholyte micelles the aggregation number grows faster than $1/Z_{net}$, and the micellar charge increases with decreasing net charge per chain. Therefore the larger values of the potential and the osmotic regime correspond to smaller net charge per chain.

5.3 Other Types of Micelles

Star-like micelles in the polyelectrolyte and osmotic regimes are stable over a wide range of the parameters, such as the fraction of charged monomers on the blocks and the net charge per chain. In addition to these two types of micelles, other micellar structures can be stable in solution. The unrestricted model predicts the existence of unusual micelles. Due to the disproportionation of chains

in the polyampholyte micelles, small aggregates need not be star-like [31]. If the net charge of the micelle epZ_{net} is smaller than the charge of the longer block eN_+f, the core of the micelles is stabilized by only two blocks partially extended into the corona. However, the regime of such "double-tailed" micelles is very narrow and could be difficult to observe experimentally.

The aggregation number of double-tailed micelles increases with decreasing net charge of a chain eZ_{net} and eventually the net charge of the micelle epZ_{net} becomes equal to the charge of the two longer blocks. The corona of the micelles with higher net charge consists of more than two chains corresponding to the star-like polyelectrolyte regime, see Sect. 5.2. If the polyampholyte diblocks are weakly charged (f is small), the decrease of the net charge per chain results in an increase of the core size rather than in the increase of the electrostatic potential because of the larger number of chains that are completely contained within the core. In this case the micellar core is of the order of the micellar size and the micelles are called "crew-cut". The electrostatic potential of these micelles is smaller than k_BT, therefore their counterions remain free in solution and the crew-cut micelles are in the polyelectrolyte regime.

Micelles made of diblock polyampholytes with strongly charged blocks are larger than those with weakly charged blocks due to the stronger attraction between oppositely charged blocks. The decrease of Z_{net} leads to an increase of the electrostatic potential and therefore to the counterion confinement within micelles. At a net charge per chain smaller than Z^*_{net} given by (51) star-like osmotic micelles are present in solution.

In the framework of the unrestricted model, the micellar cores are spherical. For the morphological transitions to other geometries (cylindrical micelles or bilayers) to occur, the core blocks have to be strongly stretched [24, 41]. Since the chains in the micelle are disproportionated between the core and corona, the core blocks are not stretched because most of the chains are completely confined to the core and are therefore not deformed. This implies that the shape transitions do not take place for disproportionated block polyampholyte micelles. This feature places the polyampholyte micelles into a unique class of aggregates.

5.4 Stability of the Micelles

Solutions of charge-symmetric diblock polyampholytes are unstable and undergo phase separation [47]. The polyampholyte micelles are made of charge-asymmetric diblocks, so the uncompensated charge ensures their stability. Nevertheless, the micelles can precipitate at non-zero net charge if the chemical potential of a chain in the micelle is higher than the chemical potential of a chain in the sediment.

A chain in the sediment interacts with other chains via fluctuation-induced attraction. The bulk contribution to the chemical potential, see (39) is the same for all aggregated structures, so it does not affect the stability boundary.

The other two contributions are the entropy of a chain and the entropy of $\Delta N f$ counterions per chain confined to the sediment. The former term is much smaller than the latter one and can be neglected. Therefore, the stability of the solution of polyampholyte micelles is mainly determined by the entropy of counterions.

Polyampholyte micelles (both star-like and crew-cut) in the polyelectrolyte regime are always stable. This stability is due to the entropy of the counterions which is much larger in the dilute supernatant than in the dense sediment. Star-like osmotic micelles are also stable because the counterions confined to a star-like micelle still have a larger volume to explore than the ones in the sediment.

The star-like osmotic micelles in the unrestricted model remain stable even if the net charge of a block polyampholyte is as low as one elementary charge. This remarkable stability is due to the partitioning of the chains and can be explained by the fact that even in this limiting case the corona of the equilibrium micelle is much larger than the core [31].

The unrestricted model predicts that charge-asymmetric block polyampholytes will not precipitate, but rather form micelles with disproportionated chains. This prediction is, however, applicable to the case of monodisperse charge distribution, i.e., if all chains carry the same net charge. Charge polydispersity will shift the region of stability of a homogeneous micellar solution. For example, a situation with an average of one elementary charge per chain can be realized by mixing positively charged, negatively charged and uncharged chains. In this case neutral and mutually neutralized fraction of oppositely charged chains would precipitate and only the fraction carrying the total net polymer charge will remain in soluble micelles.

6 Summary and Potential Applications

The increasing number of theoretical and experimental studies concerning micellization of charged block copolymers reflects growing interest in these systems both academically and in view of industrial applications. In the present chapter we have reviewed the scaling models of micelle formation in dilute solutions of diblock copolymers consisting either of hydrophobic and polyelectrolyte or of oppositely charged blocks. Most commonly the micelles are spherical star-like aggregates with a dense core and a solvated corona. A certain number of diblock copolymers are held together in the micelle by the attractive interactions in the micellar core. The origin of this attraction is different in the two systems. In the case of uncharged-polyelectrolyte diblocks the effective attraction arises from the selectively poor solvent quality for the uncharged blocks. Diblock polyampholytes interact via the charge density fluctuation-induced electrostatic attraction between oppositely charged blocks. The driving force for micellization is a reduction of the surface tension between the collapsed blocks in the core and the solvent. Stabilization

of the micelles which prevents them from unrestricted growth is assured by the electrostatic repulsion between like-charged blocks in the micellar corona. The interactions in the corona are similar in the two systems and resemble the interactions in a polyelectrolyte star.

In our review we have demonstrated that different types of interactions in the micellar core result in a number of properties different in the two types of micellar solutions. The main structural feature of polyampholyte micelles is a disproportionation of chain conformations. The chains in a micelle divide into two populations: some of them are completely confined to the core and others having entire strongly charged blocks in the corona. Such arrangement of the chains corresponds to the largest distance between like-charged monomers and therefore to the lowest electrostatic contribution to the total free energy of the micelle.

As a consequence of this disproportionation, the dependence of the micellar aggregation number on the net charge per chain eZ_{net} is stronger in polyampholyte micelles. As Z_{net} decreases the electrostatic repulsion between chains in the corona weakens, leading to an increase of the aggregation number for the two types of micelles. In polyampholyte micelles, however, there is an additional factor increasing the aggregation number with decreasing Z_{net}, namely an increase of the number of chains completely confined to the micellar core. As a result of faster growth of polyampholyte micelles their electrostatic potential increases with decreasing Z_{net} in contrast to a decrease of the potential of the polyelectrolyte micelles. Such behavior of the potential results in the different order of the polyelectrolyte and osmotic regimes in the diagram of states: in a solution of polyelectrolyte micelles an increase of net charge per chain leads to the crossover from the polyelectrolyte to the osmotic regime whereas in a solution of polyampholyte micelles the sequence of regimes is reversed.

The disproportionation also influences the stability of spherical micelles. The large number of blocks in the core of the polyampholyte micelle are not grafted to the surface of its core and therefore they are not stretched even in micelles with a very large aggregation number. In contrast to polyampholyte micelles, core blocks in polyelectrolyte micelles become stretched causing shape transitions to cylindrical and planar aggregates.

Solutions of micelles made of uncharged-polyelectrolyte block copolymers have been intensively investigated theoretically and experimentally during the past decade. Most of the studies have focused on the micellar structure as a function of molecular characteristics such as the fraction of dissociated groups in the polyelectrolyte block, the degree of polymerization, and the relative lengths of the blocks. Modern synthesis allows us to obtain block copolymers with well defined characteristics, hence the relationships between the chemical composition and the micellar properties can be well established. The theory operating with the molecular characteristics as parameters helps to steer the experimental studies which would lead to important technological applications. These applications will be based on the fact that various materials can

be placed inside the micellar core. For example, micelles can be utilized for a delivery of a drug to regions disrupted by a tumor [49]. Micelles can also be used as "nanoreactors" to produce metal or semiconductor particles [50].

While polyelectrolyte micelles have been widely studied and a good agreement between theory and experiment has been demonstrated, experimental data on block polyampholyte micelles are still limited to a few studies. Lack of data is explained by the difficulties in the synthesis of block polyampholytes with a controlled charge on each block, and by the large number of parameters governing the system behavior. Nevertheless, this field is rapidly developing, driven by the growing scientific and industrial interest in these systems. The interest is based on the unique properties of block polyampholytes which lead to a variety of applications, most importantly biomedical [51,52]. The fact that both blocks of the polyampholyte are water soluble and the core of the micelles contains electrical charges makes polyampholyte micelles a perfect vehicle for drug delivery, because various charged substances such as ions, proteins, and nucleic acids could be selectively concentrated in the core held there by electrostatic interactions. Enzymes inside the aggregates are segregated from the outer phase and therefore remain active even under unfavorable conditions outside. The other principal advantage of polyampholyte block copolymers is that it is possible to regulate the charge and, therefore, the association and stabilization behavior of the micelles. The enhanced stability of the micelles against precipitation in solutions away from the isoelectric point may be advantageously used in industry.

7 Perspectives

In the present review we have described the structural properties of spherical micelles made of linear block copolymers. Nevertheless, the possibilities for the design of novel structures are endless. Developments in synthetic chemistry and the increasing number of characterization techniques open perspectives for studying micellization in solutions of comb copolymers, H-shape, and star-shape copolymers as well as combinations of these architectures.

Block copolymer micelles are very promising systems because of the variety of possible ways to control their structure [25]. The practical way to regulate the magnitude and sign of charge in the polyampholyte solutions is to change the solution pH. Polyampholyte diblock copolymers with blocks that are hydrophobic in the absence of charge form "reversible" micelles [53, 54]. Depending on whether pH range is acidic or basic, one block is uncharged while the other is either positively or negatively charged. Therefore, the charge of the corona can be reversed by changing pH. Even richer solution behavior is observed in triblock polyampholytes with a neutral hydrophilic block [55–58], or with an oppositely charged block between two like-charged blocks [59]. The new molecular structures lead to micelles with a core, a shell and a corona, and to networks with reversible cross-links.

The notion of disproportionation, introduced for micelles formed by diblock polyampholytes can be applied to other polyampholyte systems. A simpler, yet conceptually similar, object is a polyampholyte star made of a fixed number of diblock polyampholytes [60]. Such stars may be obtained by micellization in aqueous solution of triblock copolymers with two oppositely charged blocks and one neutral hydrophobic block attached to one of the charged blocks. At a temperature lower than the glass transition temperature for the neutral block the core of the micelle is frozen and the aggregation number remains unchanged. In the polyampholyte star, the core-shell structure can be formed within it. Depending on the block charge asymmetry, solutions of polyampholyte stars may exhibit the properties of either stable colloidal solutions, or solutions with a precipitation threshold.

The existing model for micellization of diblock polyampholytes [31] explains many of their properties and describes the micellar structure in great detail. However, the simplifying assumption of equal charging of the two blocks does not allow the direct comparison with experiment. Many polyelectrolytes are weak acids or bases, so their degree of dissociation is a function of the solution pH. To improve the model one needs to consider the aggregation behaviour in the solution of block polyampholytes with the blocks having different degree of dissociation. In fact, the problem is more general and can be traced back to the solutions of oppositely charged polyelectrolytes. Despite a number of experimental studies, see [61] and references therein, the stability of soluble complexes of polyanions and polycations solutions at finite concentrations still remains an open question.

To summarize, extensive theoretical effort is desired to elucidate the interactions resulting in stable multimolecular structures in the solutions of polyelectrolytes and polyampholytes. Extensive computer simulations would test the analytical models and help to analyze the properties of real systems.

Acknowledgement. N. S. would like to thank Prof. P. Linse for a critical reading of the manuscript. M.R. acknowledges financial support of the NASA University Research, Engineering, and Technology Institute on Biologically Inspired Materials award NCC-1-02037, National Science Foundation awards CHE-0616925 and NIRT CBET-060987, as well as National Institutes of Health award 1R01HL077546-01A2.

References

1. P.-G. de Gennes: *Scaling Concepts in Polymer Physics*, (Cornell University Press, Ithaca, 1979)
2. A. Yu. Grosberg, A. R. Khokhlov: *Statistical Physics of Macromolecules*, (American Institut of Physics, New York, 1994)
3. M. Rubinstein, R. H. Colby: *Polymer Physics*, (Oxford University Press, New York, 2003)
4. J. Rühe, M. Ballauff, M. Biesalski, P. Dziezok, F. Gröhn, D. Johannsmann, N. Houbenov, N. Hugenberg, R. Konradi, S. Minko, M. Motornov, R. R. Netz, M.

Schmidt, C. Seidel, M. Stamm, T. Stephan, D. Usov, H. Zhang: Polyelectrolyte Brushes. In: *Polyelectrolytes with Defined Molecular Architecture I*, vol. 165, ed by M. Schmidt (Springer, Berlin Heidelberg New York 2004) pp 79-150
5. C. Holm, T. Hoffmann, J. F. Joanny, K. Kremer, R. R. Netz, P. Reineker, C. Seidel, T. A. Vilgis, R. G. Winkler: Polyelectrolyte Theory. In: *Polyelectrolytes with Defined Molecular Architecture II*, vol. 166, ed by M. Schmidt (Springer, Berlin Heidelberg New York 2004) pp 67-112
6. A. V. Dobrynin, M. Rubinstein: Prog. Pol. Sci. **30**, 1049 (2005)
7. J. Bohrisch, C. D. Eisenbach, W. Jaeger, H. Mori, A. H. E. Müller, M. Rehahn, C. Schaller, S. Traser, P. Wittmeyer: New Polyelectrolyte Architectures. In: *Polyelectrolytes with Defined Molecular Architecture I*, vol. 165, ed by M. Schmidt (Springer, Berlin Heidelberg New York 2004) pp 1-42
8. M. Daoud, J. P. Cotton: J. Phys. **43**, 531 (1982)
9. O. V. Borisov: J. Phys. II France **6**, 1 (1996)
10. F. Oosawa: *Polyelectrolytes*, (M. Dekker, New York, 1970)
11. P. Pincus: Macromolecules *24*, 2912 (1991)
12. J.N. Israelachvili: *Intermolecular and Surface Forces*, (Academic Press, London, 1992)
13. G. Riess: Prog. Polym. Sci. **28**, 1107 (2003)
14. G. Riess, G. Hurtrez, P. Bahadur: Block copolymers, 2nd ed. In: *Encyclopedia of Polymer Science and Engineering*, vol. 2, (Wiley, New York 1985) pp 324-434
15. I. W. Hamley: *The physics of block copolymers* (Oxford University Press, 1998)
16. J. Selb, Y. Gallot: Makromol. Chem. **181**, 809 (1980)
17. L. F. Zhang, A. Eisenberg: Science **268**, 1728 (1995)
18. K. Khougaz, I. Astafieva, X. F. Zhong, A. Eisenberg: Macromolecules **28**, 6055 (1995)
19. P. Guenoun, F. Muller, M. Delsanti, L. Auvray, Y. J. Chen, J. W. Mays, M. Tirrel: Phy. Rev. Lett **81**, 3872 (1998)
20. W. Groenewegen, A. Lapp, S. U. Egelhaaf, J. R. C. van der Maarel: Macromolecules **33**, 3283 (2000)
21. N. P. Shusharina, I. A. Nyrkova, A. R. Khokhlov: Macromolecules **29**, 3167 (1996)
22. N. P. Shusharina, P. Linse, A. R. Khokhlov: Macromolecules **33**, 3892 (2000)
23. O. V. Borisov, E. B. Zhulina: Macromolecules **35**, 4472 (2002)
24. O. V. Borisov, E. B. Zhulina: Macromolecules **36**, 10029 (2003)
25. A. V. Dobrynin, R. H. Colby, M. Rubinstein: J. Polym. Sci. B **42** (2004)
26. A. B. Lowe, C. L. McCormick: Chem. Rev. **102**, 4177 (2002)
27. S. E. Kudaibergenov: Adv. Polym. Sci. **144**, 115 (1999)
28. T. Goloub, A. de Keizer, M. A. Cohen Stuart: Macromolecules **32**, 8441 (1999)
29. J. F. Gohy, S. Creutz, M. Garcia, B. Mahltig, M. Stamm, R. Jerome: Macromolecules **33** 6378 (2000)
30. M. Castelnovo, J. F. Joanny: Macromolecules **35**, 4531 (2002)
31. N. P. Shusharina, E. B. Zhulina, A. V. Dobrynin, M. Rubinstein: Macromolecules *38*, 8870 (2005)
32. P. G. de Gennes, P. Pincus, R. M. Velasco, F. Brochard: J. Phys. **37**, 1461 (1976)
33. M. Roger, P. Guenoun, F. Muller, L. Belloni, M. Delsanti: Eur. Phys. J. E, **9**, 313 (2002)
34. G. S. Manning: J. Chem. Phys. **51**, 924 (1969)

35. Q. Liao, A. V. Dobrynin, M. Rubinstein: Macromolecules **36**, 3399 (2003)
36. M. Castelnovo, P. Sens, J. F. Joanny: Eur. Phys. J. E **1**, 115 (2000)
37. Q. Liao, A. V. Dobrynin, M. Rubinstein: Macromolecules **36**, 3386 (2003)
38. L. K. Wolterink, F. A. M. Leermakers, G. J. Fleer, L. K. Koopal, E. B. Zhulina, O. V. Borisov: Macromolecules **32**, 2365 (1999)
39. A. Jusufi, C. N. Likos, H. Löwen: J. Chem. Phys. **116**, 11011 (2002)
40. W. Groenewegen, A. Lapp, S. U. Egelhaaf, J. R. C. van der Maarel: Macromolecules **33**, 4080 (2000)
41. E. B. Zhulina, M. Adam, I. LaRue, S. S. Sheiko, M. Rubinstein: Macromolecules *38*, 5330 (2005)
42. Z. Tuzar, V. Petrus, P. Kratochvil: Die Makromol. Chem. **175**, 3181 (1974)
43. Z. Zhou, B. Chu, D. G. Peiffer: Macromolecules **26**, 1876 (1993)
44. K. Khougas, Z. Gao, A. Eisenberg: Macromolecules **27**, 6341 (1994)
45. Z. Gao, A. Eisenberg: Macromolecules **26**, 7353 (1993)
46. S. Förster, V. Abetz, A. H. E. Müller: Polyelectrolyte block copolymer micelles In: *Polyelectrolytes with Defined Molecular Architecture II*, vol. 166, ed by M. Schmidt (Springer, Berlin Heidelberg New York 2004) pp 173-210
47. V. Y. Borue, I. Y. Erukhimovich: Macromolecules *23*, 3625 (1990)
48. M. Castelnovo, J. F. Joanny: Eur. Phys. J. E *6*, 377 (2001)
49. A. Harada, K. Kataoka: Adv. Drug Delivery Rev. **16**, 295 (1995)
50. M. Antonietti, S. Förster, J. Hartmann, S. Oesteich: Macromolecules **29**, 3800 (1996)
51. A. Harada, K. Kataoka: Macromolecular Symposia **172**, 1 (2001)
52. K. Kataoka, A. Harada, Y. Nagasaki: Advanced Drug Delivery Reviews **47** 113 (2001)
53. S. Liu, S. P. Armes: Angewandte Chemie. International Edition **41**, 1413 (2002)
54. G. Hadjikallis, S. C. Hajiyannakou, M. Vamvakaki, C. S. Patrickios: Polymer **43**, 7269 (2002)
55. C. S. Patrickios, W. R. Hertler, N. L. Abbot, T. A. Hatton: Macromolecules **27**, 930 (1994)
56. W. Y. Chen, P. Alexandridis, C. K. Su, C. S. Patrickios, W. R. Hertler, T. A. Hatton: Macromolecules **28**, 8604 (1995)
57. C. S. Patrickios, L. R. Sharma, S. P. Armes, N. C. Billingham: Langmuir **15**, 1613 (1999)
58. R. Bieringer, V. Abetz, A. H. E. Müller: Europ. Phys. J. E **5**, 5 (2001)
59. V. Sfika, C. Tsitsilianis: Macromolecules **36**, 4983 (2003)
60. A. Akinchina, N. P. Shusharina, P. Linse: Langmuir **20**, 10351 (2004)
61. A. F. Thünemann, M. Müller, H. Dautzenberg, J. F. Joanny, H. Löwen: Polyelectrolyte complexes. In: *Polyelectrolytes with Defined Molecular Architecture II*, vol. 166, ed by M. Schmidt (Springer, Berlin Heidelberg New York 2004) pp 113-172